FFI-rapport 2012/01274

Rotoboost Heat Exchanger

Kristoffer Wingstedt and Øyvind Andreassen

Norwegian Defence Research Establishment (FFI)

22 November 2012

FFI-rapport 2012/01274

379001

P: ISBN 978-82-464-2169-8
E: ISBN 978-82-464-2170-4

Keywords

Varmeveksler

Roterende strømning

Kompressibel strømning

“Large Eddy Simulation”

Approved by

Bjørn Anders P. Reif	Project Manager
Jan Ivar Botnan	Director

English summary

In this report the fluid dynamical aspects of a rotating heat exchanger have been investigated. This work is a continuation of the work by Andreassen (2012) and in this report we emphasize on numerical computations on a initial design suggestion from Rotoboost AS. To briefly summarize, the rotating heat exchanger is a fast rotating centrifuge (a circumferential velocity of 360 $[\mathrm{m/s}]$) and it is intended to be an integrated part of an industrial application developed by Rotoboost AS.

The main task in this report is to investigate whether the given specifications, such as geometry and rotational speed, will suffice for an efficient heat exchanger. Results in this report indicates that the high rotational speed will suppress turbulence and, in turn, will most likely yield a low efficient heat exchanger. We stress that the results in this report are based on a specific geometry and the flow characteristics are, as well as the heat transfer process, dependent of choice of geometry. Thus, with a different geometry (and possibly a lower rotational speed) the overall conclusion may differ from that given in this report.

Sammendrag

I denne rapporten diskuteres de fluid dynamiske aspektene til rotating heat exchanger. Arbeidet er en fortsettelse av en tidligere studie av Andreassen (2012). I denne rapporten presenteres numeriske simuleringer på et design foreslått av Rotoboost AS. Kort oppsummert så er rotating heat exchanger en hurtig roterende sentrifuge (periferihastighet $360[\mathrm{m/s}]$) og intensjonen er at den skal utgjøre en integrert del av et industrielt system utviklet av Rotoboost AS.

Hovedmålet med studiet tilknyttet denne rapporten er å undersøke hvorvidt de gitte spesifikasjoner som geometri og turtall, vil utgjøre fundamentet for en effektiv varmeveksler. Resultatene presentert i denne rapporten indikerer at en høy rotasjonsrate vil undertrykke turbulens og mest sannsynlig resultere i en lite effektiv varmeveksler. Vi gjør oppmerksom på at resultatene i denne rapporten er basert på en spesifikk geometri og flow karakteristikk i tillegg til en spesifisert prosess for varmetransport som avhenger av valg av geometri. Vi tar forbehold om at konklusjonen kunne blitt annerledes for en geometri som er forskjellig fra den som er spesifisert og for en lavere rotasjonsrate.

Contents

Preface

Rotoboost AS have demonstrated that the efficiency of electrolysis is strongly enhanced when an artificial “gravitational” field is applied. In electrolysis, gas bubbles are formed in a fluid. Increased buoyancy due to the increased gravity (rotation) will increase the efficiency in separating the bubbles from the fluid. The efficiency increases with rotation rate. There is a need for a heat exchanger in this process and the idea has been to connect the heat exchanger to the apparatus that does the electrolysis. That implies a cylindrically shaped and rotating heat exchanger with the same rotation rate as the system for electrolysis. We have asked the question whether the heat exchanger will gain or loose efficiency when run at high rotation rates.

Nomenclature

Greek letters

α	Thermal diffusivity, $\alpha = \frac{k}{\rho c_p}$, $[\mathrm{m}^2/\mathrm{s}]$
$\rho 2\boldsymbol{\Omega} \times \boldsymbol{u}$	Coriolis force (per unit mass) [N]
β	Thermal expansion coefficient $[1/\mathrm{K}]$
γ	Heat capacity ration, c_p/c_v (dimensionless)
Λ	Compression factor
ρ	Density $[\mathrm{kg}/\mathrm{m}^3]$
ν	Kinematic viscosity, $\nu = \frac{\mu}{\rho}$, $[\mathrm{m}^2/\mathrm{s}]$
$\rho\boldsymbol{\Omega} \times (\boldsymbol{\Omega} \times \boldsymbol{r})$	Centrifugal force (per unit mass)[N]
$\boldsymbol{\Omega}$	Constant rotation vector, $\boldsymbol{\Omega} := (0, 0, \Omega)$, $[\mathrm{rad}/\mathrm{s}]$
Ω	Rotation rate $[\mathrm{rad}/\mathrm{s}]$
$\boldsymbol{\omega}$	Vorticity vector, $\boldsymbol{\omega} := \nabla \times \boldsymbol{u}$

Roman letters

A	Area $[\mathrm{m}^2]$
c_p	Specific heat capacity $[\mathrm{J}/\mathrm{Kg\ K}]$
$\boldsymbol{e}_z$	Axial unit vector
h	Convective heat transfer coefficient $[\mathrm{W}/\mathrm{m}^2]$
$\mathcal{L}$	Characteristic length scale [m]
p	Fluid pressure [Pa]
$p^\star$	Reduced fluid pressure [Pa]
q	Convective heat transfer $[\mathrm{Wm}^2]$
R	Universal gas constant $[\mathrm{J}/\mathrm{kg\ K}]$
$\boldsymbol{r}$	Position vector, $\boldsymbol{r} = (r, \varphi, z)$
Re	Reynolds number, $\mathrm{Re} = \frac{\mathcal{U}\mathcal{L}}{\nu}$ (dimensionless)
Ri	Richardson number, $\mathrm{Ri} = g\left(\frac{g(\gamma-1)}{C^2} - \frac{1}{T}\frac{\partial T}{\partial r}\right)/\left(\frac{\partial U_r}{\partial r}\right)^2$ (dimensionless)
Ro	Rossby number, $\mathrm{Ro} = \frac{\mathcal{U}}{\Omega\mathcal{L}}$ (dimensionless)
T	Temperature [K]
$\triangle T$	Temperature difference [K]
$\mathcal{U}$	Characteristic velocity $[\mathrm{m}/\mathrm{s}]$
$\boldsymbol{U}$	Mean fluid velocity vector $[\mathrm{m}/\mathrm{s}]$
U_r	Mean radial component $[\mathrm{m}/\mathrm{s}]$
U_z	Mean axial component $[\mathrm{m}/\mathrm{s}]$
$\boldsymbol{u}$	Fluid velocity vector $[\mathrm{m}/\mathrm{s}]$
u_r	Radial velocity component $[\mathrm{m}/\mathrm{s}]$
u_z	Axial velocity component $[\mathrm{m}/\mathrm{s}]$
u_r^{rms}	Root mean square (rms) radial component $[\mathrm{m}/\mathrm{s}]$
u_z^{rms}	Root mean square (rms) axial component $[\mathrm{m}/\mathrm{s}]$

1 Introduction

A heat exchanger is a piece of equipment built for efficient heat transfer from one fluid (i.e. gas or liquid) to another. In most cases, the fluids are separated by a solid wall and the hot and the cold fluids never mix. Energy exchange is thus accomplished from one fluid to the surface by convection, through the wall by conduction, and then by convection from the wall to the second fluid. The rotating heat exchanger is based on the idea of a fast rotating centrifuge where the heat transfer between the hot fluid and the cold fluid is mainly located at the outer rim of the centrifuge. In the initial design concepts, it is suggested that the circumferential velocity is to be set to 360 $[\mathrm{m/s}]$, which is beyond the speed of sound in air. The high circumferential velocity is motivated by the fact that the rotating heat exchanger is to be integrated as a part of an industrial application subjected to high rotation.

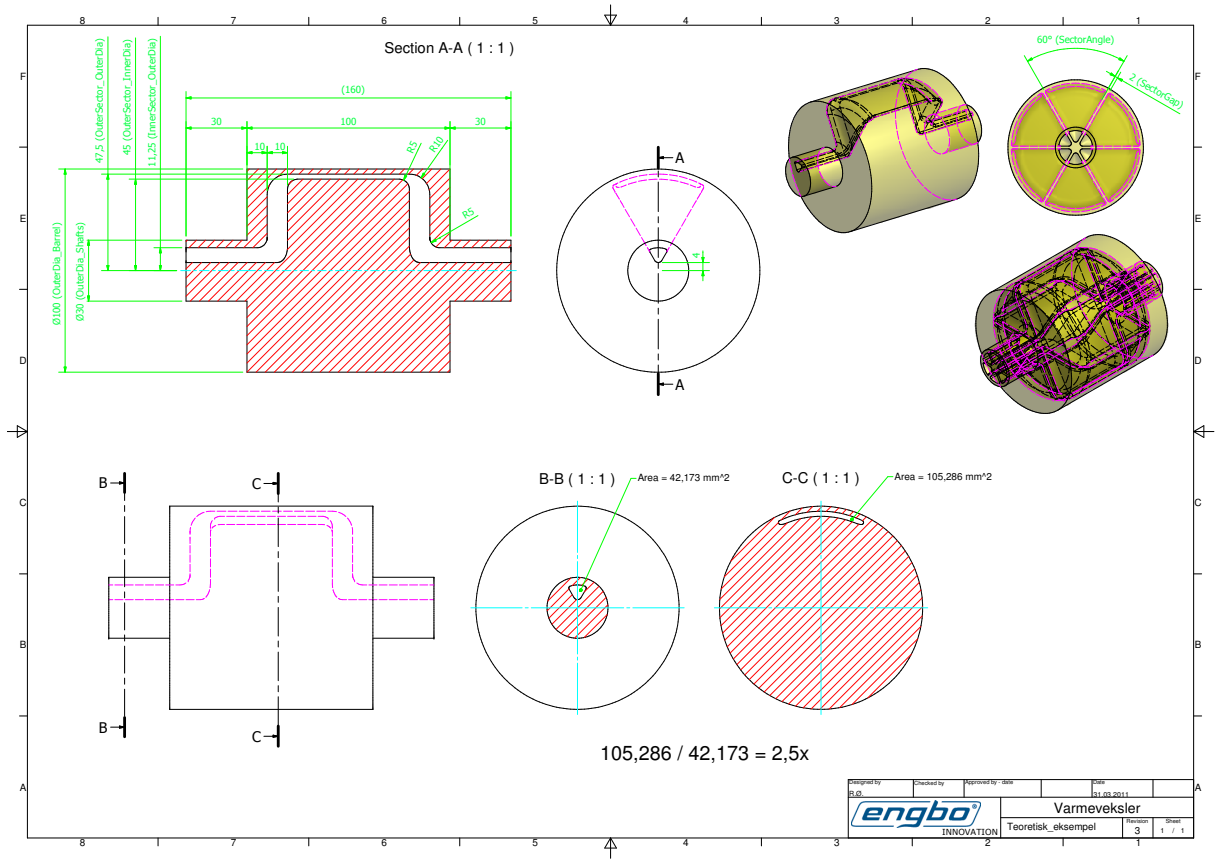

Figure 1.1 A concept design of the rotating heat exchanger. In this initial design only one channel is present.

The corresponding heat exchange between the hot and cold fluid is highly dependent of the behavior of the fluids in the centrifuge. From the rotation of the centrifuge, a strong "gravitational force" (commonly denoted fictive gravitation) will effect the fluids as they are passed through channels that radially expands from the inlet, located close to the center line of the centrifuge, to the outer rim, see Figure 1.1. This fictive gravitation has two contributions; a so-called Coriolis

force and a centrifugal force. The latter can be identified as a body force potential and can be treated as a part of modified pressure. Increased centrifugal force will reduce convective mixing. The Coriolis force which is dependent on the rotation rate and the radial velocity component of the fluid (we may neglect the effects of the azimuthal velocity component) has a tendency to suppress turbulence. This follows from the famous Taylor-Proudman theorem.

In this report we focus on the fluid dynamical aspects of the flow that is located in the outer rim of the centrifuge, which is motivated by the idea that a significant part of the heat exchange will occur in this region, which implies that the flow tends towards a two-dimensional state in a plane perpendicular to the rotation axis. Turbulence can not persist in two dimensions.

2 Basic principles of convective heat transfer

In this section we consider a brief introduction of the basic mechanisms for heat transfer in context and application to heat exchangers.

Energy exchange and heat transfer between a solid surface and an adjacent fluid is called convective[1] heat transfer. The rate of convection in such a case is formally given by the equation

$$q = h \triangle T \, A \tag{2.1}$$

which is sometimes referred to as the Newton rate equation. Here, q is the rate of convective heat transfer, h is the convective heat transfer coefficient, $\triangle T$ is the temperature difference of the solid surface and the fluid and A is the area where the convective heat transfer occurs. It should be noted that a "fluid" could be a gas or a liquid. We also note that (2.1) is not a physical law, but rather a definition of the convective heat transfer coefficient h. In general, we distinguish between two classifications of convective heat transfer; natural convection and forced convection. The most effective way to transport heat by convection in a fluid is by forced convection where the heat is transported by the bulk movement of the fluid. In such a process, the heat transport is driven by fluid velocity fluctuations that is driven by an "external unit", such as a fan or a pump, that produce a fluctuating bulk movement. In such a case, the convective heat transfer coefficient in (2.1) is highly (and non-linearly) dependent of the property of the flow. To determine the convective heat transfer coefficient for forced convection is not a trivial task. There exist many quantitative and empirical formulas in literature that estimates h and the corresponding correlations (coupling) between momentum, heat and mass transfer, see Welty et al. (2001). Most of these formulas are derived by dimension analysis where the convective heat transfer coefficient is dependent on several different dimensionless numbers such as the Nusselt, Prandtl, Grashof, Rayleigh, and the Reynolds number. However, by estimating the different timescales for different

[1] The term convection may have slightly different but related usages in different scientific or engineering contexts or applications. The broader sense is in fluid mechanics, where convection refers to the motion of fluid regardless of cause. However, in thermodynamics "convection" often refers specifically to heat transfer by convection. Additionally, convection includes fluid movement both by bulk motion (advection) and by the motion of individual particles (diffusion).

flow regimes (and here we only distinguish between laminar and turbulent flows), we can relate the speed of propagation of the corresponding temperature distribution by means of the Reynolds number $\mathrm{Re} = \frac{\mathcal{U}\mathcal{L}}{\nu}$. The Reynolds number physically signifies the ratio between inertial and viscous forces acting on the fluid and it is the most common dimensionless number used in fluid mechanics.

If we start by considering the case with a laminar flow we assume that the fluctuating bulk velocity is negligible. In this case the heat transfer is dominated by molecular diffusion and the corresponding temporal temperature distribution $T(\boldsymbol{x}, t)$ can be approximated by the diffusion equation and in terms of orders of magnitude,

$$\frac{\partial T}{\partial t} = \nabla \cdot (\alpha \nabla T) \quad \Leftrightarrow \quad \frac{T}{\tau_M} \sim \alpha \frac{T}{\mathcal{L}^2}. \tag{2.2}$$

Using (2.2), we can estimate the order of magnitude of the molecular diffusive timescale τ_M as

$$\tau_M \sim \frac{\mathcal{L}^2}{\alpha}, \tag{2.3}$$

for some length scale $\mathcal{L}$ and for some constant thermal diffusivity α. That is, the timescale of diffusion is given by the independent parameters of $\mathcal{L}$ and α. If we now consider the case of a turbulent flow characterized by the same length scale $\mathcal{L}$; that is, the motions that are present are of length scales $\leq \mathcal{L}$, with a characteristic velocity of $\mathcal{U}$, we obtain the characteristic turbulent diffusion timescale

$$\tau_T \sim \frac{\mathcal{L}}{\mathcal{U}}. \tag{2.4}$$

The characteristic velocity $\mathcal{U}$ in (2.4) is to be considered as the root mean square (rms) of the velocity fluctuations in the turbulent flow. If we, without any loss of generality, consider air where $\nu/\alpha = 0.73$[2] and divide (2.3) with (2.4) we obtain the ratio of the different timescales as

$$\frac{\tau_M}{\tau_T} \sim 0.73\ \mathrm{Re} \sim \mathrm{Re}. \tag{2.5}$$

From (2.5) we see that molecular diffusive timescale is a factor Re larger than the turbulent timescale, which is in general several orders of magnitude. Thus, a heat transfer process driven by a turbulent flow is a factor Re more efficient than that of laminar flow. This analysis illustrates that *heat transfer is much more efficient in turbulent flows than laminar flows*. In terms of heat exchanger design, the presence of turbulence will enhance the efficiency of the heat exchanger and is a wanted state of the fluid flow.

Remark. A heat transfer process driven by natural convection is a process wherein the bulk motion of the fluid results from the heat transfer. When a fluid is heated or cooled, the associated density change and buoyancy produce a natural circulation which affect the fluid that moves past the solid surface. A convective unstable flow is usually also strongly turbulent and heat transfer in a convective unstable flow is very efficient. Much more efficient compared to molecular diffusive

[2] We note that the ration $\nu/\alpha = \mathrm{Pr}$ where Pr is the Prandtl number. The Prandtl number for gases are of unit size whereas for liquids the Prandtl number is about 10.

heat transfer that occurs in laminar flows. After all, convection is a result of strong temperature differences and convection is the most efficient mechanism known to reduce the temperature difference. For a gas in a gravitational field, there is an upper limit on how big a temperature difference can be before convective processes will neutralize it. Shear will increase the possibility for flow instabilities. A stability criteria based on a combination of shear and convection if considered in section 5.3.2.

3 Governing equations

In this section we present the formal mathematical formulation of the problems that are associated with the rotating heat exchanger. Moreover, we present analytical results for (incompressible) fluids subjected to high rotation rates. For a more in comprehensive discussion on fluids subjected to rotation see Greenspan (1969); Childs (2011).

3.1 Fluid equations

The fluid problem that are associated with the rotating heat exchanger are described by the compressible (Newtonian) Navier–Stokes equations. As mentioned earlier, the rotating heat exchanger is rotating about the rotation axis, see figure 3.1, and in such a case it is convenient to write the Navier–Stokes equations in a non-inert (rotating) frame of reference. In such as coordinate system, the relative[3] velocity is given by $\boldsymbol{u} = (u_r(r,\varphi,z,t), u_\varphi(r,\varphi,z,t), u_z(r,\varphi,z,t))$, the pressure $p = p(r,\varphi,z,t)$, the density $\rho = \rho(r,\varphi,z,t)$ and the temperature $T = T(r,\varphi,z,t)$ where (r,φ,z) are the radial, tangent and axial coordinates, respectively. If we assume a constant angular velocity around the rotation axis, i.e., $\boldsymbol{\Omega} = (0,0,\Omega_z) := (0,0,\Omega)$, we can write[4] Navier–Stokes equations on the component form[5]:

$$\frac{D\rho}{Dt} + \rho\Lambda = 0 \tag{3.1a}$$

$$\begin{aligned}
\rho\Big(\frac{Du_r}{Dt} - \frac{u_\varphi^2}{r}\Big) &= -\frac{\partial p}{\partial r} + \frac{1}{3}\mu\frac{\partial \Lambda}{\partial r} + \mu\Big(\boldsymbol{\nabla}^2 u_r - \frac{u_r}{r^2} - \frac{2}{r^2}\frac{\partial u_\varphi}{\partial \varphi}\Big) + \rho g_r \qquad (3.1b)\\
&\quad +2\Omega\rho u_\varphi + \rho\Omega^2 r\\
\rho\Big(\frac{Du_\varphi}{Dt} + \frac{u_r u_\varphi}{r}\Big) &= -\frac{\partial p}{r\,\partial \varphi} + \frac{1}{3}\mu\frac{\partial \Lambda}{r\,\partial \varphi} + \mu\Big(\boldsymbol{\nabla}^2 u_\varphi - \frac{u_\varphi}{r^2} + \frac{2}{r^2}\frac{\partial u_r}{\partial \varphi}\Big) + \rho g_\varphi \qquad (3.1c)\\
&\quad -2\Omega\rho u_r\\
\rho\Big(\frac{Du_z}{Dt}\Big) &= -\frac{\partial p}{\partial z} + \frac{1}{3}\mu\frac{\partial \Lambda}{\partial z} + \mu\boldsymbol{\nabla}^2 u_z + \rho g_z \qquad (3.1d)
\end{aligned}$$

$$\begin{aligned}
\rho c_p\Big(\frac{DT}{Dt}\Big) &= \beta\frac{Dp}{Dt} + k\boldsymbol{\nabla}^2 T - \frac{2}{3}\mu\Lambda^2 \qquad (3.1e)\\
&+ \mu\Big(2(\Phi_{rr}^2 + \Phi_{\varphi\varphi}^2 + \Phi_{zz}^2) + \Phi_{\varphi z}^2 + \Phi_{rz}^2 + \Phi_{r\varphi}^2\Big).
\end{aligned}$$

Here, (3.1a), (3.1b) - (3.1c), and (3.1e) are the continuity, momentum and energy equations, respectively. The continuity equation describes the conservation of mass where $\Lambda = \nabla \cdot \mathbf{v}$ is the

[3] The terms "absolute" and "relative" are common use in fluid mechanics and the are associated with a fluid velocity and accelerations in a stationary (inertial) or a rotating (non-inertial) frame of reference, respectively.

[4] For a formal derivation of the momentum equation in a moving reference frame, see Batchelor (1967). Moreover, the compressible Navier–Stokes equations in a cylindrical coordinate system can be found in many text books, see e.g. Hinze (1975) and White (1991).

[5] See Appendix A for further details regarding all mathematical operators present in (3.1a)-(3.1e).

compression factor. In (3.1b)-(3.1d) the three components of the momentum equation are given, governed by Newton's second law of motion. We note that in the radial direction (3.1b), three "additional" terms are present due to the system rotation: u_r^2/r, $2\Omega\rho u_\varphi$ and $\rho\Omega^2 r$. The first term is usually denoted relative acceleration which is the acceleration observed in a non-inertial frame of reference. The second term is the so-called Coriolis force and the third term is the centrifugal force. These two last terms are commonly denoted fictitious forces and they appear (as well as the relative acceleration) as a consequence of the relative fluid velocity formulation where the momentum equation is formulated in a so-called non-inertial reference frame. A non-inertial frame of reference is a frame of reference that is undergoing acceleration with respect to an inertial frame which in this case is a cylindrical coordinate system rotating about the axial coordinate with a constant angular velocity Ω. The effect of theses fictitious force will be further investigated in section 3.2. It should be kept in mind, however, that these two terms do not represent actual forces but are rather kinematic consequences of viewing the motion from a rotating frame of reference. Furthermore, we also notice that the tangential component of the momentum equation (3.1c) has a relative acceleration $u_r u_\varphi/r$ and a Coriolis force $2\Omega\rho u_r$, but lacks a centrifugal force term. Moreover, since we consider a constant angular rotation around the rotation axis, we have no kinematic contributions in the axial direction (3.1d). Finally, the energy equation (3.1e) describes the temperature distribution in the fluid which is governed by the first law of thermodynamics. We consider an ideal gas where the density ρ, the pressure p and the static temperature T are linked by the equation of state $p = \rho RT$, where R is the universal gas constant. Moreover, β is the thermal expansion which is $1/T$ for an ideal gas, and Φ is the thermal dissipation of heat.

3.2 Analytical considerations on flows subjected to rotation

In this section we present analytical results for flows subjected to high rotation rates. The governing set of equations in the previous section (i.e. the compressible Navier–Stokes) can in some cases be simplified and analytically analyzed, by qualitative arguments. This is to be considered as an addition to Andreassen (2012) where the analysis is extended on the isothermal and incompressible flow properties for fluids subjected to a high rotation rate. Since we consider the isothermal incompressible case, the energy equation (3.1e) will be disregarded in this section. Moreover, due to the assumption of an incompressible fluid, the compression factor $\Lambda = 0$. **Remark.** We stress that the results presented in this section, we do not consider nor treat the turbulent nature of rotating flows. In this section we make qualitative estimates on how the different forces arising from rotation act on fluid flows. Later, in section 5.3.1, we will address the implications of turbulence and its effect on rotating flows in connection with the presented numerical simulations on the rotating heat exchanger.

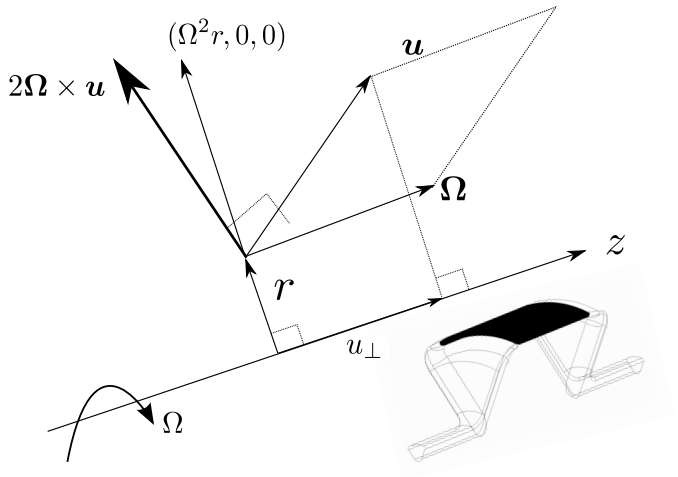

Figure 3.1 Illustration of the Coriolis forces and centrifugal forces in the case of a constant rotation about the rotation axis z. In bottom right corner a picture of the concept design of the rotating heat exchanger is depicted for orientation.

To get a better overview of the analysis in this section, we write (with a slight abuse of notation) the corresponding incompressible versions of (3.1a)-(3.1d) on a the compact form[6]

$$\nabla \cdot \boldsymbol{u} = 0 \tag{3.2}$$

$$\frac{\partial \boldsymbol{u}}{\partial t} + (\boldsymbol{u} \cdot \nabla)\boldsymbol{u} = -\frac{1}{\rho}\nabla p + \nu \Delta \boldsymbol{u} - 2\boldsymbol{\Omega} \times \boldsymbol{u} - \boldsymbol{\Omega} \times (\boldsymbol{\Omega} \times \boldsymbol{r}), \tag{3.3}$$

where $\nu = \mu/\rho$ is the kinematic viscosity and $\boldsymbol{r} = (r, \varphi, z)$. Given this set of equations, we see that the Coriolis term is given by $2\boldsymbol{\Omega} \times \boldsymbol{u}$. Thus, the Coriolis force is perpendicular to the angular velocity vector and the (relative) velocity vector with a magnitude of $2\Omega u_\perp$ where $u_\perp$ is the component of the velocity perpendicular to the axis of rotation, see figure 3.1. The term $\boldsymbol{\Omega} \times (\boldsymbol{\Omega} \times \boldsymbol{r})$ is the centrifugal force which points in the radial direction with magnitude $\Omega^2 r$, see figure 3.1. For a fluid with uniform density, it is convenient to combine the (modified) pressure with centrifugal force to form the so-called reduced pressure gradient, where the reduced pressure gradient $\nabla p^\star$ is given by[7]

$$\nabla p^\star = \nabla p - \frac{1}{2}\nabla((\boldsymbol{\Omega} \times \boldsymbol{r}) \cdot (\boldsymbol{\Omega} \times \boldsymbol{r})). \tag{3.4}$$

Using the reduced pressure we can write the momentum equation (3.3) as

$$\frac{\partial \boldsymbol{u}}{\partial t} + (\boldsymbol{u} \cdot \nabla)\boldsymbol{u} = -\frac{1}{\rho}\nabla p^\star + \nu \Delta \boldsymbol{u} - 2\boldsymbol{\Omega} \times \boldsymbol{u}. \tag{3.5}$$

[6]For a fluid with uniform density, it customary to incorporate the gravity in the pressure term which is called the modified pressure which is still denoted p. This modified pressure arises wholly from the effect of motion of the fluid, determined by the equation (3.3).

[7]In our case the rotation vector is $\boldsymbol{\Omega} = (0, 0, \Omega)$ and thus $\boldsymbol{\Omega} \times (\boldsymbol{\Omega} \times \boldsymbol{r}) = -\Omega^2 r \boldsymbol{e}_r$, where $\boldsymbol{e}_r$ is the radial unit vector. Hence the centrifugal force only acts on the reduced pressure gradient in the radial direction as illustrated in figure 3.1. Moreover, we can write the reduced pressure as $\nabla p^\star = \nabla(p - \frac{1}{2}\Omega^2 r^2)$, where r is the distance from the axis of rotation.

The reason for introducing the reduced pressure is that we can relate the effect of the centrifugal force as to that of the pressure gradient. However, the effect of the Coriolis force and how it changes the character of the flow is not obvious in flows with complex geometries.

3.2.1 The stabilizing effect of the Coriolis force

When effects of rotation is dominant (i.e. when then Coriolis force dominates the inertial force) fluid motions exhibits properties quite different form those with no rotation. In order to define this regime it is necessary to define a measure of the importance of the rotational effect on the fluid. If we consider a steady flow ($\partial \boldsymbol{u}/\partial t = 0$), where we let $\mathcal{U}$ and $\mathcal{L}$ denote the characteristic velocity and length scales, we can write the dimensionless momentum equation (3.5) as

$$\left[\frac{\mathcal{U}}{\Omega\mathcal{L}}\right](\tilde{\boldsymbol{u}} \cdot \nabla)\tilde{\boldsymbol{u}} = -\nabla p^{\star} + \left[\frac{\nu}{\Omega\mathcal{L}^2}\right]\Delta\tilde{\boldsymbol{u}} - 2\boldsymbol{e}_z \times \tilde{\boldsymbol{u}}, \tag{3.6}$$

where $(\tilde{})$ denotes non-dimensional variables and $\boldsymbol{e}_z$ is the unit vector in the direction of the axis of rotation. The two dimensionless terms in the brackets are parameters that characterize the importance of the rotation and viscous force respectively.

The parameter $\mathcal{U}/\Omega\mathcal{L}$ gives a measure of the ratio of (relative) inertial forces to Coriolis forces (or, equivalently, relative flow acceleration to Coriolis acceleration). This dimensionless parameter is known as the Rossby number, Ro[8]. As we can see from the definition of the Rossby number, a fluid flow with a high rotation speed we have $\mathrm{Ro} << 1$ and the Coriolis force suppress the inertial forces. The second term $\nu/\Omega\mathcal{L}^2$ is referred to as the Ekman number, Ek, and it measures the ratio between viscous forces and Coriolis forces. For a small Ekman number, $\mathrm{Ek} << 1$, we can expect a thin viscous layers in the flow. We note that the ratio between the Rossby number and the Ekman number gives the Reynolds number; that is, $\mathrm{Ro}/\mathrm{Ek} = \mathrm{Re} = \mathcal{U}\mathcal{L}/\nu$.

If we now assume a high rotation speed and a high Reynolds number, such that $\Omega >> \mathcal{U}/\mathcal{L}$ and $\mathrm{Re} >> 1$, we can approximate (3.6) with the inviscid equation

$$-\frac{1}{\rho}\nabla p^{\star} = 2\boldsymbol{e}_z \times \tilde{\boldsymbol{u}}. \tag{3.7}$$

This approximation indicates that for a flow dominated by rotation, the Coriolis force is balanced by the pressure gradient. If we go one step further and take the curl of (3.7) and use the continuity equation (3.2), we obtain

$$(\boldsymbol{e}_z \cdot \nabla)\tilde{\boldsymbol{u}} = 0. \tag{3.8}$$

From (3.8) we can conclude that there is no spatial variation of the velocity field in the direction parallel to the axis of rotation. This results is referred to the Taylor-Proudman theorem and the flow can be regarded as a two dimensional flow. Since the flow parallel to axis of rotation is

[8]The Rossby number is mostly used in meteorological flow applications where the Rossby number is far greater than that of our application. However, as we shall see below, it is quite convenient to use the Rossby number in the context of equation (3.6). It should be mentioned that in many engineering applications (such as in turbo machinery) the inverse of the Rossby number, the so-called Rotational number $\mathrm{N} = \frac{\Omega\mathcal{L}}{\mathcal{U}}$, is used.

constant, *the net effect of the Coriolis force is that it stabilizes the flow*. Equations (3.7) - (3.8) indicates that some of the most important effects of incompressible fluids subjected to high rotational speeds can be accounted for by this (yet simple) preliminary analytic analysis. However, the two dimensionality is broken when solid boundaries are present (like in the rotating heat exchanger).

3.2.2 The effect on the relative vorticity in rotational flows

The stated Taylor-Proudman theorem gives us the information that in rotating flows, for low enough Rossby and Ekman numbers, the flow can be consider two dimensional due to the Coriolis force acting on the fluid. In order to see how the Coriolis force effect the vorticity of the flow, $\boldsymbol{\omega} := \nabla \times \boldsymbol{u}$, we take the curl of (3.5) and obtain the vorticity equation

$$\frac{\partial \boldsymbol{\omega}}{\partial t} - \nabla \times (\boldsymbol{u} \times \boldsymbol{\omega}) = \nu \Delta \boldsymbol{\omega} + (2\boldsymbol{\Omega} \cdot \nabla)\boldsymbol{u}. \tag{3.9}$$

If we again consider the steady inviscid version of (3.9), we have

$$-\nabla \times (\boldsymbol{u} \times \boldsymbol{\omega}) = (2\boldsymbol{\Omega} \cdot \nabla)\boldsymbol{u}. \tag{3.10}$$

We interpret the left-hand side of (3.10) as the rate of (spatial) change of the (relative) vorticity. By the Taylor-Proudman theorem, the right-hand side describes the change in magnitude and direction of the background vorticity ($2\boldsymbol{\Omega}$) associated with the variations of the (relative) velocity field along the direction of the axis of rotation. If we now let $\mathcal{L}$ denote the length scale of the flow variation along the axis of rotation and $\mathcal{U}$ the characteristic velocity the Coriolis force on the right-hand side in (3.10) has the order of magnitude $2\Omega\mathcal{U}/\mathcal{L}$. For the left-hand side, we can approximate the order of magnitude to be $\mathcal{U}^2/\mathcal{L}^2$. If we recall the definition of the Rossby number, we can approximate the ratio between the left-hand side and the right-hand side of (3.10) as

$$\mathrm{Ro} = \frac{\mathcal{U}}{\Omega\mathcal{L}} \sim \frac{\mathcal{U}^2/\mathcal{L}^2}{2\Omega\mathcal{U}/\mathcal{L}} \approx \frac{|\nabla \times (\boldsymbol{u} \times \boldsymbol{\omega})|}{|(2\boldsymbol{\Omega} \cdot \nabla)\boldsymbol{u}|} \sim \frac{|\boldsymbol{\omega}|}{\Omega}. \tag{3.11}$$

Hence, we see that the Rossby number can be approximately interpreted as the ratio between the (relative) vorticity of the fluid and the rotational speed. Given the estimate in (3.11) we can expect that the vorticity along the axis of rotation is can be neglected when a fluid is subjected to a high rotational rate. This analysis shows, in agreement with the Taylor-Proudman theorem, that a fluid subjected to a high rotation rate will be stabilized due to the (high) Coriolis force.

4 Numerical approach

In this section we describe the basics of the numerical methods that are used in the simulations of the rotating heat exchanger which are presented in section 5.

It is well known that, up to this date, there does not exist any analytical solutions to the Navier–Stokes equations for arbitrary initial data and boundary conditions. That is, in order to extend the analysis in section 3.2, we most conduct numerical simulations on the rotating heat exchanger. All the numerical simulations presented in this report are performed with the commercial code ANSYS FLUENT 13.0. This code is one of the most widely used software package in engineering to simulate and evaluate fluid flow related problems which are commonly referred to as Computational Fluid Dynamics (CFD). ANSYS utilize the finite volume method where the spatial computational domain consist of a finite number of computational cells ("volumes") and the temporal discretization is solved by a finite difference method, see for instance Versteeg and Malalasekera (1995). The computational cells can have different geometrical shapes (simplexes), such as hexagons or tetrahedrons, while the temporal discretization (i.e. the dynamic evolution of the corresponding discretized equations) can be either solved using an implicit method or an explicit method. The accuracy of the obtained results from such simulations are highly dependent on the spatial and temporal resolution of the simulations. The resolution is given by the computational grid size (or mesh size), whilst the temporal resolution is given by the time-step size. Moreover, in CFD there are generally two distinct ways to solve the numerical equations stemming form the spatial and temporal discretization; by a Direct Numerical Simulation (DNS) or by a using a suitable turbulence model.

A DNS is a numerical simulation in which the Navier–Stokes equations are numerically solved without any turbulence model. This means that the whole range of spatial and temporal scales of the turbulence must be resolved. All the spatial scales of the turbulence must be resolved in the computational mesh, from the smallest dissipative scales (the so-called Kolmogorov scales) to the large scales associated with the motions containing most of the kinetic energy. This type of simulations are not common in engineering applications since it requires a very fine spatial (and thus temporal) resolution of the computational grid. It is easy to estimate the resolution necessary for such computations for given Reynolds number Re. If we let n denote the number of grid points along one spatial direction, one must fulfill the constraint in a three dimensional simulation, that the number of grid points $N = n^3 \geq \mathrm{Re}^{9/4}$, which is far to many grid points to be handle even with current years most powerful supercomputers for a flow problem with a moderate Reynolds number.

The only possible approach to simulate high Reynolds number (i.e. turbulent) flows is to apply an appropriate turbulence model for the finer scales, rather than to resolve them in the computational grid. There exist a great number of different models with associated sub models and modifications therein. However, roughly speaking, there exist two main classes of turbulence models; the Reynolds Averaged Navier–Stokes (RANS) models and Large Eddy Simulation (LES) models.

In the RANS approach, the velocity and pressure fields are decomposed using a so-called Reynolds decomposition where the instantaneous fields are the sum of a mean field and a fluctuating field. After plugging in this decomposition into the (instantaneous) Navier–Stokes equations and averaging, an ensemble-averaged equation for the mean flow is obtained (which is the Navier–Stokes equation for the mean velocity and mean pressure) plus an additional (nonlinear) term accounting for the effect of the fluctuating velocity on the mean flow. This term is referred to as the Reynolds stress and this term introduces new unknown variables which in turn leads to a closure problem. The heart of RANS modeling is to model the Reynolds stress by different techniques (such as two-equations models, algebraic models etc.) and the most widely used models in engineering applications are the so-called $K - \epsilon$ type of models. For a quick overview of the basic RANS models, see for instance Wilcox et al. (1998).

All the presented simulations in this report are computed using the LES approach and we will briefly explain this technique below.

4.1 LES - Large Eddy Simulation

The goal of the LES computational technique is first and foremost to compute the large energy containing eddies (structures) in the flow. The scales that are computed are referred to as the resolved scales and the size of such scales are directly linked to the spatial and temporal resolution of the computational domain. To define the size of theses scales, one starts with applying a filter to the Navier–Stokes equations. There are several ways of doing this mathematically and all are essentially equivalent to averaging the equation over a small region of space (which is equivalent to low-pass filtering the equation in Fourier space[9]). These small regions are then defined by the present grid size of the computational domain. For a compressible flow, the typical filter that is used in LES is the so-called Favré filter (Garnier et al., 2009; Grinstein et al., 2007) where the variables are filtered using a density time average. Formally, the Favré average is mathematically a change of variables[10] and this type of average is used in FLUENT for compressible LES computations (FLUENT, 2011). This type of filter does not commute with the nonlinear convective term in the Navier–Stokes equations and this leads to an unresolved small scale term which needs to be modeled. The common name for theses types of models are Sub Grid Scale models, or SGS for short.

In all of our simulations, we have chosen the so-called dynamic Smagorinsky–Lilly SGS model. The concept of the dynamic procedure is to apply a second filter (called a test filter) to the equations of motion. The new filter width is equal to twice the grid filter width. Both filters produce a resolved flow field. The difference between the two resolved fields is the contribution of the small scales whose size is in between the grid filter and the test filter. The information related to these scales is used to compute the so-called dynamic Smagorinsky constant which is used as a part of

[9] See Garnier et al. (2009) for a more comprehensive discussion of different types of LES filters.

[10] In a compressible flow, the "main variable" to solve is the momentum $\rho \boldsymbol{u}$ in contrast to the incompressible case where the main variable is the velocity $\boldsymbol{u}$. In order to avoid an additional sub grid scale model to the continuity equation for compressible flow, the Favré averaging is used.

the model.

In the simulations to come, we frequently refer to mean quantities and root mean square (rms) quantities. The mean velocity $\boldsymbol{U}$ (the first moment) is formally defined (for a Favré averaged velocity) as

$$\boldsymbol{U} = \lim_{T\to\infty} \int_{t'}^{t'+T} \frac{1}{\overline{\rho}} \rho \hat{\boldsymbol{u}} \, \mathrm{d}t, \tag{4.1}$$

where $\overline{\rho}$ denotes the time average density and $\hat{\boldsymbol{u}}$ the resolved velocity field. Deviation from the mean velocity field is given by the rms (the second moment) and is defined as

$$\boldsymbol{u}^{\mathrm{rms}} = \lim_{T\to\infty} \sqrt{\int_{t'}^{t'+T} \left(\frac{1}{\overline{\rho}} \, \rho \hat{\boldsymbol{u}} - \boldsymbol{U} \right)^2 \mathrm{d}t}. \tag{4.2}$$

Moreover, the mean velocity can also be averaged over a region of space and, for example, the mean axial velocity component is denoted $\langle \boldsymbol{U} \rangle_z$ and it is defined as

$$\langle \boldsymbol{U} \rangle_z = \int_0^{z'} \boldsymbol{U} \, \mathrm{d}z. \tag{4.3}$$

Remark. As mentioned above, the most conventional approach for solving CFD problems are by using some type of $K-\epsilon$ model. However, the standard $K-\epsilon$ model are incapable of modeling and predicting the main physical features of turbulent flows subjected to rotation. The reason is that the model utilize a scalar representation of the turbulent field. For a more comprehensive discussion on this matter, see Speziale et al. (2000).

5 Simulations

In this section we present the simulations on the rotating heat exchanger.

5.1 Restrictions

As mentioned in the introduction, we restrict our numerical simulations to the outer rim of the channel, see figure 5.1. Moreover, we only consider isothermal boundary conditions; that is, we set the temperature at the channel wall to be equal to that of the fluid. We motivate these restriction by:

i) In the extension, when two channels are present, a significant part of the heat exchange will occur in this region, and the behavior of the flow in this section is very important for the heat transfer process, see discussion in section 2

ii) We can estimate the effect of temperature gradients on the wall by theory for stratified flows, see section 5.3.2

With the above restrictions we can isolate the problem and thus reduce the parameter space. More precisely, we hereby focus only on the flow properties in the outer rim of the centrifuge.

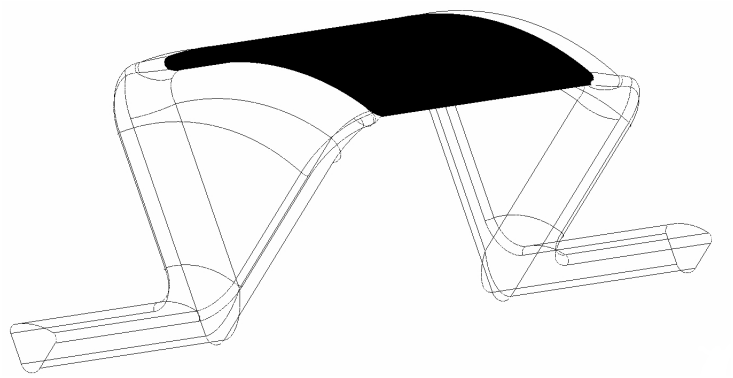

Figure 5.1 Illustration of one of the channels in the rotating heat exchanger. We restrict our simulations to the outer rim which is marked in the shaded region. Since this section is symmetric in the axial direction we can easily investigate the behavior of the mean axial flow.

5.2 Mesh generation and boundary conditions

The computational mesh consists of a structured hexagon grid which is generated with the software package ICEM CFD. The dimensions of the grid measures $50 \times 20 \times 2.5$ [mm] and consists of about 1.5×10^6 cells with facet size varying between $0.125 - 0.2$ [mm] along with a y^+–value which does not exceed 5. A pressure (drop) boundary condition is set and due to symmetry, a periodic boundary condition is set on the velocity in the axial direction. The pressure drop over the rim is set to obtain the mass flow equivalent to that of the inlet (located in the center line of the centrifuge) velocity of 50 [m/s]. Finally, we consider air at 300 [K] as medium and the boundary of the rim also given the temperature 300 [K].

5.3 Results

5.3.1 Axial velocities

We start by examine the axial flow properties where the circumferential velocity is set to 360 [m/s]. The axial flow properties are important since a large portion of convection of heat will occur along the axial direction of the outer rim. In figure 5.3 the mean and rms axial velocities, averaged in the axial direction, are depicted.

In figure 5.3, we see that mean axial velocity is asymmetric and varies from roughly 1 [m/s] in the left corner (pressure side) to about 15 [m/s] in the right corner (suction side). The asymmetric behavior is also present in the axial rms velocity. Deviations from the mean flow only occur on the pressure side and there is virtually no deviations from the mean flow else were in the outer rim. The deviations on the pressure side arises from the secondary mean flow where periodic roll-cells (called Taylor–Görtler vortices) roll along the rotation axis, see figure 5.4. One cell takes

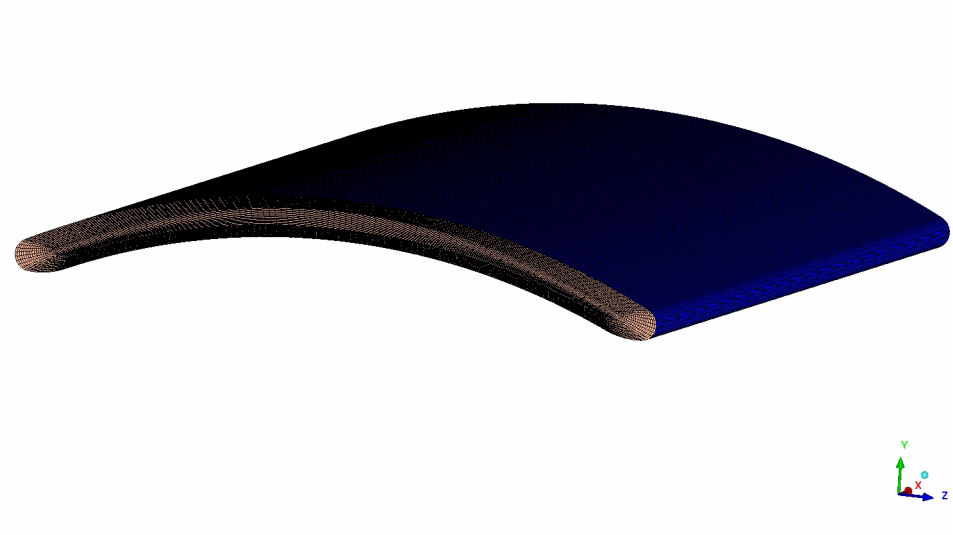

Figure 5.2 The computational mesh of the outer rim.

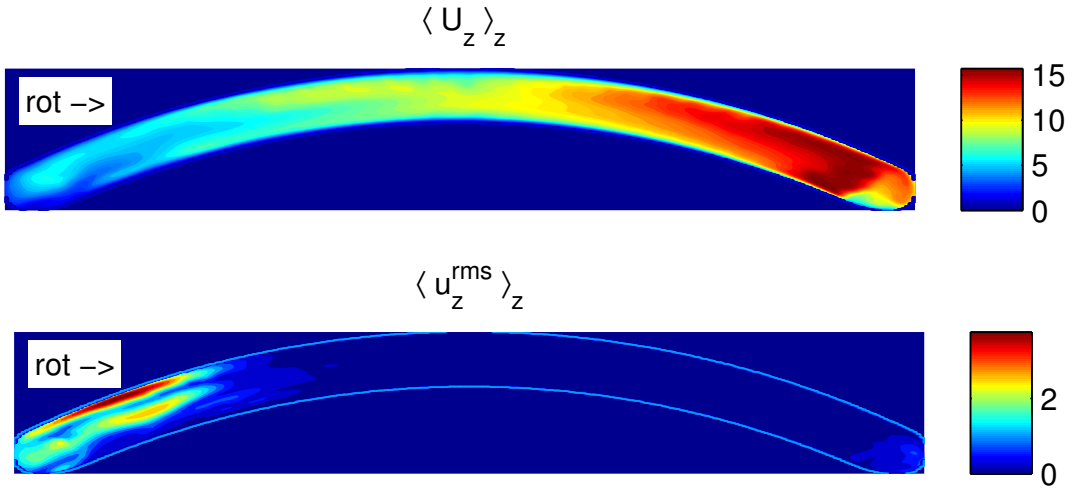

Figure 5.3 Plots of mean axial velocity $\langle U_z \rangle_z$ and axial rms velocity $\langle u_z^{rms} \rangle_z$, both average in the axial direction. Here, "rot –>" indicates the direction of rotation.

approximately 12 revelations to travel from the inlet to the outlet. This type of secondary mean flow is most likely (initially) generated by turbulence and this phenomena is called the Prandtl's first instability. This type of vortices are sustained by the combined effect of body forces and system rotation. The vortices enable large scale mixing of the flow and thus the pressure side enables transport of heat more effectively than that of the suction side. However, these vortices are only present in a small region of the outer rim. To increase the number of radial-axial walls beyond a certain number will impose constraints to the flow that will reduce mixing. There may exist an optimal number, but we believe that the effect is small.

Combining the information of the mean and rms velocities we can visualize the turbulent kinetic energy in the axial direction, q_z^2, which is shown in figure 5.5 below. Figure 5.5 clearly illustrates that the turbulent kinetic energy in the axial direction is generally low and also highly asymmetric. This indicates that in overwhelming part of the outer rim; that is, where $q_z^2 = 0$, the flow is to be consider laminar and the corresponding heat transfer in such as case is dominated by molecular diffusion. Moreover, the flow is highly asymmetric and indicates that the heat transfer in this case will be non-uniform in the rim.

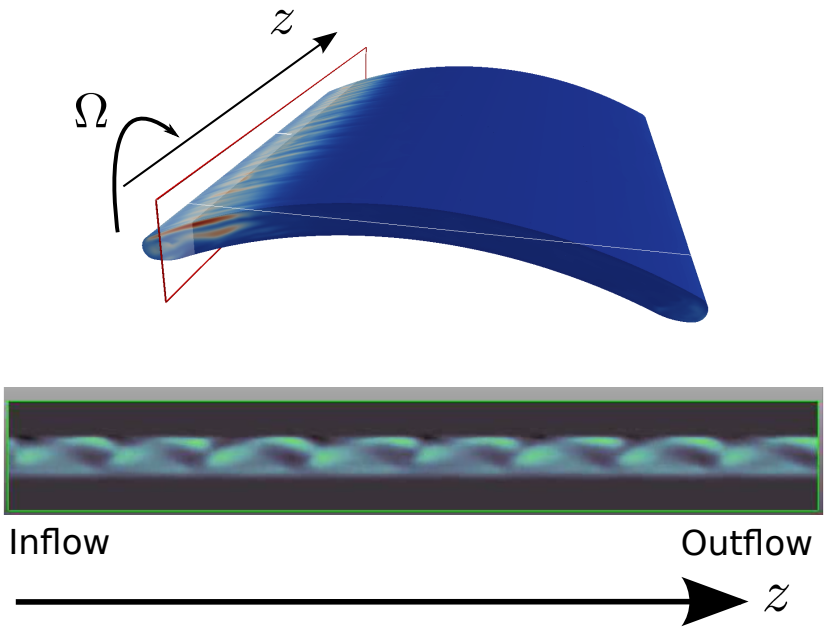

Figure 5.4 *Snapshot form one of the visualizations, see the Preface for how to obtain theses visualizations. The red bounding box on the top picture illustrates where the slice is taken along the axial axis. The lower picture shows the slice along the axial direction and illustrates the magnitude of the instantaneous (resolved) velocity component $\hat{u}_z$. Light green illustrates a high velocity magnitude (approximately $5\ [m/s]$) whilst black indicates a low velocity magnitude (approximately $0\ [m/s]$).*

Remark. As mentioned, the simulations are performed with the circumferential velocity $360\ [\mathrm{m/s}]$. This high circumferential velocity is motivated that the heat exchanger is to be in-

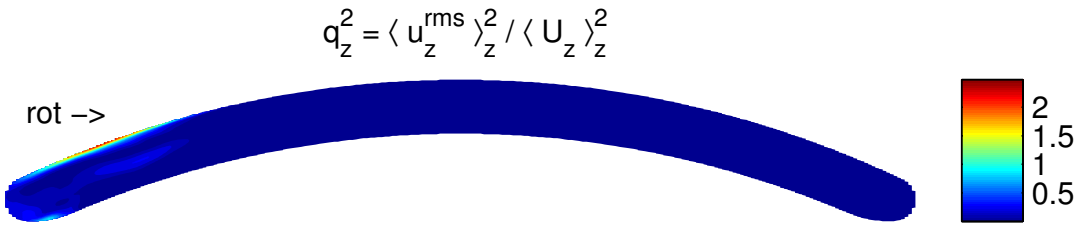

Figure 5.5 Turbulent kinetic energy in the axial direction q_z^2, averaged in axial direction.

tegrated in an industrial application subjected to this rotational speed. In connection with the result presented, we also conducted simulations on lower rotational speeds. More precisely, we simulated the rotational speeds $360/2, 360/4, 360/8$ [m/s] and the results is to be found in Appendix B. The general trend was that the axial mean flow $\langle U_z \rangle_z$ increased with decreased rotational number. Moreover, the rms axial velocity $\langle u_z^{\text{rms}} \rangle_z$ also increased with decreased rotational speed. We also noticed that both the mean and rms velocities tend to a symmetric behavior at the circumferential velocity between $450 - 414$ [m/s].

5.3.2 The Richardson number – stability analysis

The results of the simulations in section 5.3.1 where computed with isothermal wall boundary conditions. When the full heat exchanger is considered a radial temperature difference, $\partial T/\partial r$, between the flow in the outer region and the inner region will be present. If the temperature difference is high enough the density gradients can induce an unstable flow. In this case, the restoring force that should bring a fluid element out of position back to equilibrium, will act in the same direction as the motion and push it further out of equilibrium. This is called convective instability. This situation occurs when the temperature gradient is steeper than the adiabatic temperature gradient. That is when

$$\frac{\partial T}{\partial t} > \left(\frac{\partial T}{\partial r}\right)_{ad} = \frac{\Omega^2 r}{c_p} = \frac{\Omega^2 r(\gamma - 1)}{R\gamma} \tag{5.1}$$

Here R is the gas constant and $\gamma = c_p/c_v$ is the ratio of specific heats which equals $7/5$ for a two-atomic gas.

In the case studied in this report, $(\partial T/\partial r)_{ad} = 1.3 \times 10^3$K/m. In addition to the convective instability, the radial shear of the axial velocity can induce a shear instability. The most unstable situation is convection combined with a strong shear. As $\partial T/\partial r$ drops below $(\partial T/\partial r)_{ad}$, stability increases. A measure of the stability is the magnitude of the Brunt-Väisälä frequency which definition is given below, see (5.2). More info about buoyancy and buoyancy waves can be found in (Lighthill, 1978). A convectively unstable situation can occur with zero averaged flow or zero mean shear. The presence of a shear $(\partial U_z/\partial r)$ will increase the potential for instabilities and turbulence to occur. The combination of instabilities in the presence of shear and/or convection has motivated introduction of the Richardson number Ri as a stability/instability criteria. The

Brunt-Väisälä frequency is defined as follows

$$N^2 = \frac{g}{\theta}\frac{\partial \theta}{\partial r} = \frac{g}{T}\left(\left(\frac{\partial T}{\partial r}\right)_{ad} - \left(\frac{\partial T}{\partial r}\right)\right). \tag{5.2}$$

The Richardson number is defined, see for example (Drazin and Reid, 1981)), as

$$Ri = \frac{N^2}{\left(\frac{\partial U_z}{\partial r}\right)^2}, \tag{5.3}$$

where U_z is the mean axial velocity (a function of r only). The instability/stability criteria is as follows

$Ri \leq 0,$	convectively unstable
$0 < Ri \leq 1/4,$	dynamically unstable
$1/4 < Ri \leq 1,$	dynamically unstable ?
$1 < Ri,$	stably stratified

When $1/4 \leq Ri \leq 1$, Ri is a fuzzy measure and it is unclear whether the flow is stable or unstable. For $Ri > 1$ all experimental evidence indicate that the flow is stable. When $Ri >> 1$ the flow is strongly stable. That is due to high stratification (large N) or small shear or a combination of both. For large Richardson numbers, turbulence is suppressed. In the case of an isothermal fluid

$$Ri = \frac{g^2(\gamma - 1)}{TR\gamma\left(\frac{\partial U_z}{\partial r}\right)^2} = \frac{1}{c_p T}\frac{\Omega^4 r^2}{\left(\frac{\partial U_z}{\partial r}\right)^2}.$$

We see that Ri varies as $\Omega^4 r^2$. This implies that the stability strongly increases with rotation rate as long as the gas is convectively stable. Based on the maximum measured shear from the numerical simulations and assuming an isothermal fluid, we are going to estimate the most unstable Ri for the rotating heat exchanger flow.

The maximum shear measured from the numerical simulations is 1.2×10^4(m/s)/m. The adiabatic temperature gradient is 1.3×10^3K/m. For an isothermal gas the Richardson number becomes $Ri = 4 \times 10^{-2} << 0.25$. According to the stability criteria given above, *the flow is unstable and turbulence may develop*. Even though the stratification is extremely strong, the shear dominates which indicates that the flow may be turbulent.

As mentioned before that the Richardson number criteria is valid for plane and unbounded flows. A case that differs from the rotating channel flow. The Richardson number criteria may be used with care in this case. Therefore we have carried out a careful numerical study that to the contrary shows that the flow is close to laminar. The simulations show that the flow is turbulent at lower rotation rates and that there is a rotation rate limit where the flow becomes non-turbulent which is what is expected from the Richardson number criteria. The numerical study is carried out for an isothermal flow. It must be mentioned that an increasing temperature gradient will also increase instability and cause turbulence.

However, the tendency for instabilities to occur due to stratification is limited to a region in the flow where the mean velocity gradient $\partial U_z/\partial r$ is large. Towards the center at the channel $\partial U_z/\partial r \rightarrow 0$. This implies that although turbulence will develop close to the walls on both sides of the channel, there will be very little mixing across the entire channel height.

In the suction side of the rim, the mean axial velocity is almost constant in the axial direction along a constant angle which means that the flow is closely two-dimensional.

6 Concluding remarks

In this report, which is a continuation of the work by Andreassen (2012), we have investigated and evaluated by qualitative and quantitative methods the flow properties of the rotating heat exchanger. All the presented material in this report are aimed for understanding the flow properties in the heat exchanger and how they effect the heat transfer process.

The main idea behind the design of the rotating heat exchanger is that the increased centrifugal forced induced by the strong system rotation, will compress the fluids and thereby increase the temperature and, in the end, enhance the efficiency of the heat transfer process. However, after having investigated the dynamics of the flow with the given parameters such as geometry, inlet velocity and rotation rate, our simulations indicate that the heat transfer process in the rotating heat exchanger likely will have a rather low efficiency.

One of the key features for an efficient heat transfer process is to have a turbulent flow. Turbulence enables an efficient transportation of heat whilst a stable laminar flow regime is inefficient with respect to heat transport. In this report we have seen (both by analytical grounds and computational grounds) that the high rotational rates have a stabilizing effect on the flow and suppress turbulence. This effect arises from the fictitious forces, the centrifugal force and the Coriolis force, which dominate the characteristics of a flow subjected to high rotational rates. Even though all numerical computations are performed with isothermal boundary conditions and closely isothermal flows, it is uncertain whether a plausible temperature difference on the channel walls will cause turbulence. The simulations show that by reducing the rotation rates may cause the flow to become turbulent and enhance heat transfer.

We stress that the conclusions drawn from the numerical computations in this report are solely based on a specific given parameter set. If another geometry is used, the conclusions may differ. Below a certain rotation rate, the flow will be turbulent and the heat transfer will be efficient. The simulations show that the flow is turbulent for $n = 1/4$ but probably not for $n = 1/2$, see also Appendix B. A more extensive analysis is needed to reveal exactly where the turning point is.

Appendix A Operators i the Navier–Stokes equations

The scalar material derivative is defined as:

$$\frac{D(\,\cdot\,)}{Dt} = \frac{\partial(\,\cdot\,)}{\partial t} + u_r \frac{\partial(\,\cdot\,)}{\partial r} + \frac{u_\varphi}{r}\frac{\partial(\,\cdot\,)}{\partial \varphi} + u_z \frac{\partial(\,\cdot\,)}{\partial z}.$$

The scalar Laplacian is defined as:

$$\boldsymbol{\nabla}^2(\,\cdot\,) = \frac{\partial^2(\,\cdot\,)}{\partial r^2} + \frac{\partial(\,\cdot\,)}{r\,\partial r} + \frac{\partial^2(\,\cdot\,)}{r^2\,\partial \varphi^2} + \frac{\partial^2(\,\cdot\,)}{\partial z^2}.$$

The compression factor Λ is defined as:

$$\Lambda = \frac{\partial u_r}{\partial r} + \frac{u_r}{r} + \frac{\partial u_\varphi}{r\,\partial \varphi} + \frac{\partial u_z}{\partial z}.$$

Appendix B Plots at lower rotational speeds

In this section, we present simulations done on lower rotational speeds on the outer rim. All simulations presented in this section are done with the exact same parameters (model, mesh etc.) as those in section 5.3.1, except the rotational speed. We divide the circumferential speed $360\ [\mathrm{m/s}] := n$ by $2, 4, 8$, where the lowest speed is given by $n = 1/8 \Rightarrow 45\ [\mathrm{m/s}]$. The tipping point for the symmetric flow behavior is between $0.8 < n < 0.85$.

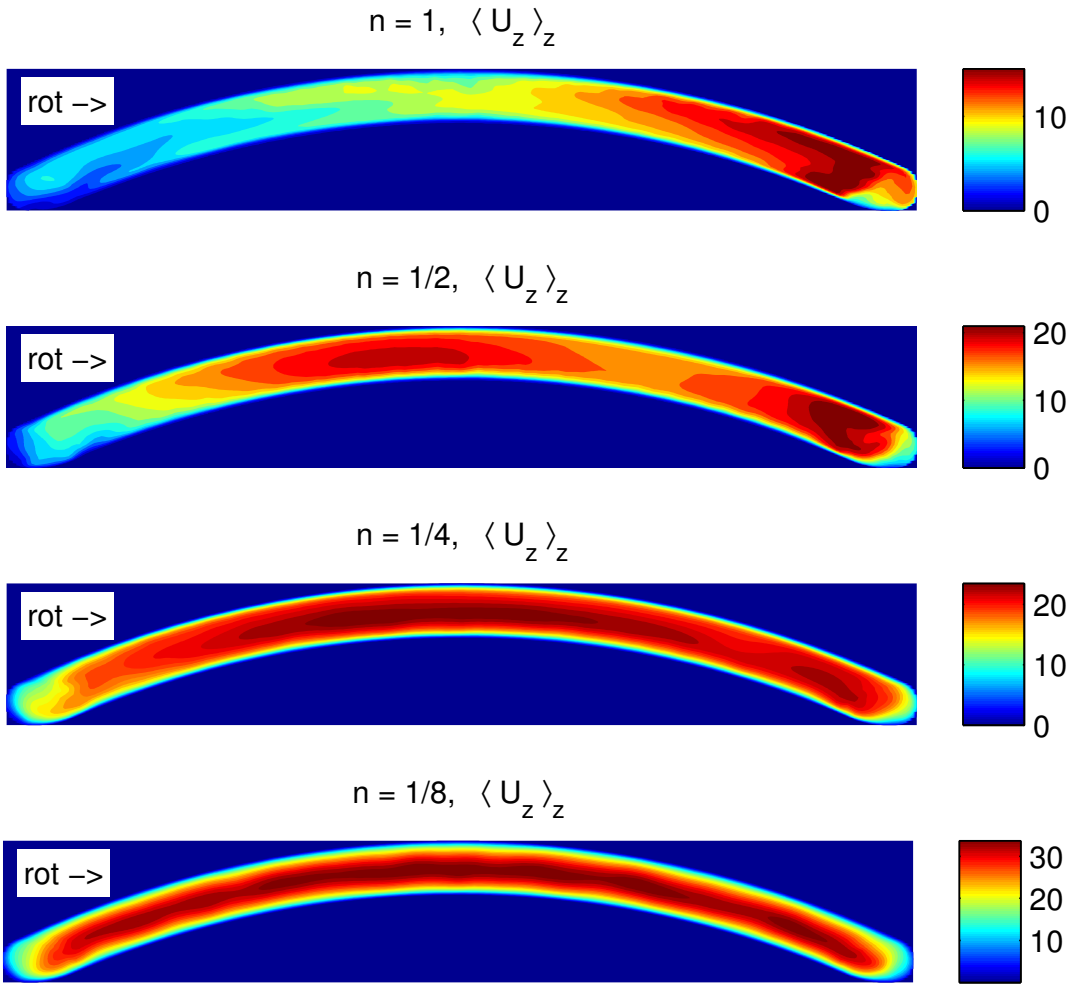

Figure B.1 *Axial mean velocity $\langle U_z \rangle_z$ for different rotation rates n, all averaged in the axial direction.*

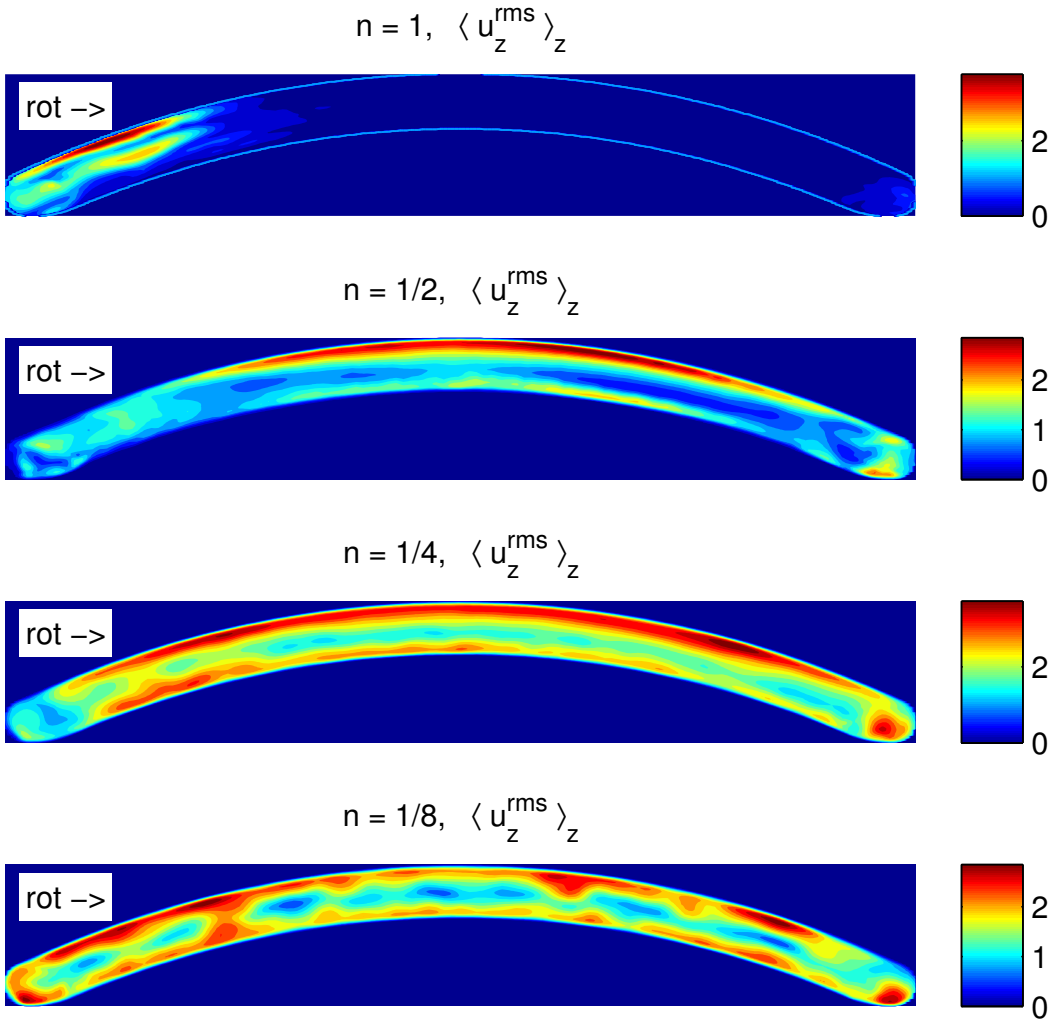

Figure B.2 Axial rms velocity $\langle u_z^{rms} \rangle_z$ for different rotation rates n, all averaged in the axial direction.

References

Ø. Andreassen. An analytical study of gas flow in a system operating at high rotation rates, the Rotoboost heat exchanger. *FFI-rapport 2012/00330*, 2012.

G.K. Batchelor. *An introduction to fluid dynamics*. Cambridge University. Cambridge. US, 1967.

P.R.N. Childs. *Rotating Flow*. Elsevier, 2011.

P. G. Drazin and W. H. Reid. *Hydrodynamic Stability*. Cambridge Monographs on Mechanics and Applied Mathematics. Cambridge University Press, Cambridge University Press, 1981.

ANSYS FLUENT. 13.0 theory guide. *ANSYS Inc*, 2011.

E. Garnier, P. Sagaut, and N. Adams. *Large eddy simulation for compressible flows*. Springer Verlag, 2009.

H.P. Greenspan. *The theory of rotating fluids*. Cambridge University Press, London, 1969.

F.F. Grinstein, L.G. Margolin, and W. Rider. *Implicit large eddy simulation: computing turbulent fluid dynamics*. Cambridge Univ Pr, 2007.

J.O. Hinze. *Turbulence (2nd edn)*. McGraw-Hiil, New York, 1975.

J. Lighthill. *Waves in fluids*. Cambridge University Press, Cambridge University Press, 1978.

C.G. Speziale, B.A. Younis, and S.A. Berger. Analysis and modelling of turbulent flow in an axially rotating pipe. *Journal of Fluid Mechanics*, 407(1):1–26, 2000.

H.K. Versteeg and W. Malalasekera. *An introduction to computational fluid dynamics: the finite volume method*. Prentice Hall, 1995.

J.R. Welty, C.E. Wicks, and R.E. Wilson. *Fundamentals of momentum, heat, and mass transfer*. John Wiley & Sons Inc, 2001.

F.M. White. *Viscous fluid flow*, volume 2. McGraw-Hill New York, 1991.

D.C. Wilcox, American Institute of Aeronautics, and Astronautics. *Turbulence modeling for CFD*, volume 2. DCW industries La Canada, CA, 1998.